



# Photometric determination of the age and distance of the open cluster NGC 2420

Francesco Bussola<sup>1</sup>, Marco Faccioli<sup>4</sup>, Giovanni Frezzato<sup>3</sup>, Giulio Romanelli<sup>2</sup>

<sup>1</sup>Liceo *Galilei*, sez. Scientifico PNI, Verona

<sup>2</sup>Liceo *Galilei*, sez. Scientifico Tradizionale, Verona

<sup>3</sup>ISIS *Calabrese-Levi*, sez. Scientifico PNI, San Pietro in Cariano

<sup>4</sup>Liceo *Medi*, sez. Scientifico Tradizionale, Villafranca di Verona

**Abstract.** The magnitudes were measured in the three colors  $g$ ,  $r$ ,  $i$  for 738 stars of the open cluster NGC 2420 using the aperture photometry technique. The images obtained with the  $g$ ,  $r$ ,  $i$  filters were taken from the SDSS archive. The  $g$ ,  $r$ ,  $i$  magnitudes were transformed in the magnitudes of the standard photometric system  $B$ ,  $V$ ,  $R$ . With the  $B$ ,  $V$ ,  $R$  magnitudes we were able to build the Color-Magnitude Diagrams (CMDs).

The aim of this work was the determination of the age and the distance of NGC 2420. By comparing the stellar distribution on a  $B-V$  vs  $V$  CMD, with the isochrones obtained from theoretical models, we were able to find these parameters. The isochrones depend on two main parameters, age and metallicity, so when the match between the stellar distribution and the isochrone is reached, we have both the parameters. Since the models were reddening free, it was possible to determine the color excess,  $E(B-V)$  and then the interstellar absorption  $A_V$ . The obtained results were compared with those found in literature, finding a substantial agreement, overall for the age and the metallicity. The age we obtained is 2 Gyr, the metallicity,  $Z$ , is between 0.004 and 0.008, the distance is about 2500 pc, and the color excess,  $E(B-V)$ , is between 0.07 and 0.16. An estimate of the radii of the stars was performed by means the surface brightness method. The stellar radius at the CMD turnoff is between 2 and 3  $R_\odot$ , which is consistent with the age of the cluster.

## 1. Introduction

An open cluster is a group of stars inner to the galactic plane and it was born from a single cloud of interstellar dust. It is composed by a small number of stars (about 700 in the case of NGC 2420), all relatively young (they belong to population I). The open cluster shows the stars distributed in a central denser region surrounded by a halo, without a well defined nucleus. As cluster dimensions are much smaller (very few light-years in diameter) than its distance from Solar System, we can assume all stars are at the same distance from the observer.

Age and distance are parameters that can be defined thanks to a Color-Magnitude Diagram (CMD). In order to build a CMD it is necessary to calculate the magnitude of the stars of the cluster at least in two spectral bands. Thus, we can get the color index (that is the difference between two magnitudes), which has to be plotted on a graph with one of the two measured magnitudes, for example:  $B-V$  vs  $V$ . On the CMD, stars are distributed in two main regions, the Main Sequence (MS) (population I, young stars) and the Asymptotic Giants Branch (AGB) (population

II, old stars). The point of passage from MS to AGB, called turnoff (Figure 1), moves downward over time, stars with advanced spectral class (low temperature) take considerably more time to trigger the burning of Helium. If we identify the turnoff point on the CMD, we can estimate the age and the distance of the cluster.

In order to determine the magnitude of a star in a specific spectral band we must measure the amount of light (the number of photons) recorded by the CCD detector and subsequently transform it into the calibrated magnitude, according to Pogson's equation:

$$m = -2.5 \times \log(I) + k \quad (1)$$

Where  $I$  is the light intensity, derived from the photons count,  $m$  the magnitude of the star and  $k$  the coefficient of calibration.

In this work, we built two CMDs,  $B-V$  vs  $V$  and  $V-R$  vs  $R$  of the cluster NGC 2420. By comparing our data with isochrones, theoretical models describing the position of stars with the same age in CMDs, we were able to determine the age, the color excess due to the absorption by interstellar dust, and the distance of the cluster. Finally, we calculated the radii of the stars and we made an estimate of the metallicity of NGC 2420.

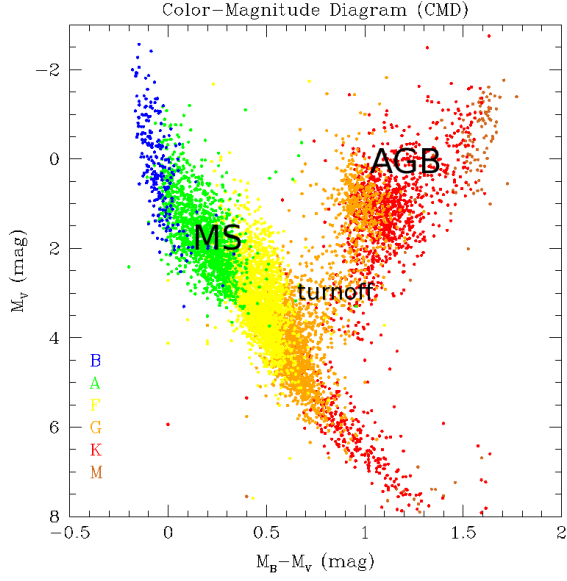


**Fig. 1.** Color-Magnitude Diagram based on the Hipparcos data, the spectral type of the stars is coded by different colors (from <http://www.astrow.edu.pl>).

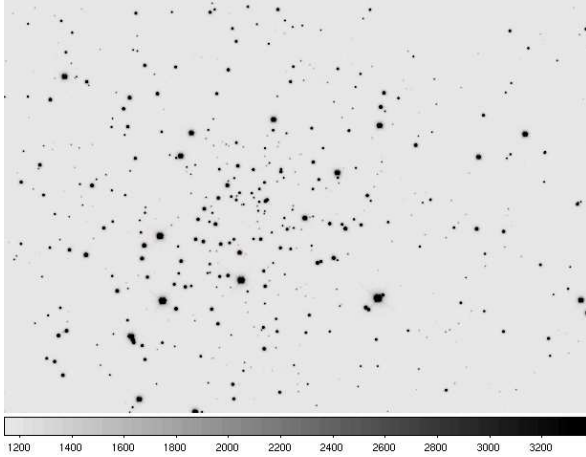


**Fig. 2.** Image of NGC 2420 taken with the  $r$  filter, SDSS.

## 2. Observational Data

Observational data were extracted from the SDSS archive (Sloan Digital Sky Survey, [www.sdss.org](http://www.sdss.org)), one of the most important ones in astronomy. The archive gets data from a 2.5-meters-wide telescope, located in Apache Point Observatory, New Mexico (USA). The field of view of the telescope is of 1.5 square degrees, which corresponds to 8 times the size of the full moon (source [www.sdss.org](http://www.sdss.org)). In this research we used images taken with the  $g$ ,  $r$ ,  $i$  filters and exposure time was 53.9 seconds for each image. In Figure 2 it is shown an image of NGC 2420, taken with the  $r$  filter.

The coordinates of NGC 2420 are  $\alpha=07^{\text{h}}.35^{\text{m}}.5^{\text{s}}$  and  $\delta=+21^{\circ}41'$ .

The atmospheric thickness value (airmass), the coefficient of atmospheric absorption ( $k$ ) and the coefficient of correction ( $m_0$ ), to convert the instrumental magnitudes, relating to the photons count, to the calibrated ones, are shown in Table 1.

Filter	airmass	$k$	$m_0$
$g$	1.07	0.14	24.447
$r$	1.06	0.09	24.071
$i$	1.06	0.03	23.741

**Table 1.** Atmospheric absorption, airmass and calibration photometric coefficient (zero-point) parameters, relating to each filter.

## 3. Work description

In order to measure the  $g$ ,  $r$  and  $i$  magnitudes of the same stars, at first it was necessary to align the three images. So, we considered the x-y positions of a sample of five stars as reference. The stars were common to every image and, after the calculation of their Cartesian coordinates, assuming the  $r$  image as reference, we calculated the  $\Delta x$  and  $\Delta y$  values of the displacement vector of the other two images (Table 2). Therefore, we shifted the  $g$  and  $i$  images so that all stars had the same coordinates.

Filter	$\Delta x$	$\Delta y$
$g$	-1.45	-11.29
$r$	0.00	0.00
$i$	1.04	-2.85

**Table 2.** X-Y shift values for the alignment of the three images.

The technique employed is the so-called aperture photometry, whose principle is to derive the energy that comes from a source by subtracting the energy of a ring of sky from the amount of energy detected in a circle concentric with the ring, containing the source. However, it is necessary that the area of the circle is equal to the one of the ring; this gives the medium value of the brightness of the sky for pixel and it is multiplied by the number of pixels in the circle, obtaining an equivalent result. So, for each image, we determined the Full Width at Half Maximum (FWHM) of the stars, the medium brightness of sky and the relative dispersion ( $\sigma$ ) of the sky-counts. In order to identify the FWHM, we chose a sample of 15 sources for each image. The source had to show a gaussian type of intensity distribution, that means a regular trend with a well-defined maximum (Figure 3); in case the source had saturated the pixels (the image is overexposed) it would not be possible to define the FWHM because, having received

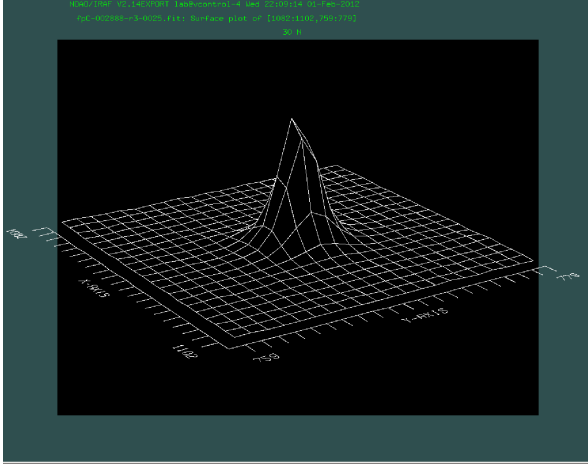


**Fig. 3.** Intensity distribution of a non-saturated source. The profile is approximated by a gaussian.

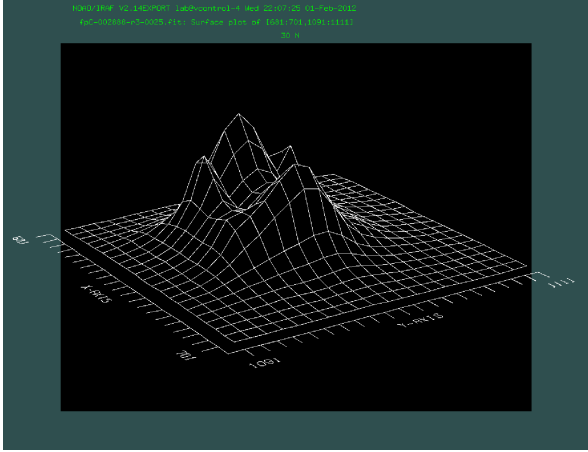


**Fig. 4.** Intensity distribution of a saturated source. The profile is absolutely irregular.

a too high number of photons, the intensity distribution recorded by the pixels is not approximated to a Gaussian (Figure 4). We considered a medium value for each of these parameters (Table 3).

Filter	FWHM (pixels)	sky counts	$\sigma$
<i>g</i>	3.33	1091.2	2.76
<i>r</i>	2.67	1150.6	5.76
<i>i</i>	2.38	1300.0	5.58

**Table 3.** FWHM and sky counts with their dispersion ( $\sigma$ ) obtained from the average of 15 stars for each image. These parameters were employed by the task DAOFIND in the automatic search for stars.

Found values served as input for IRAF task DAOFIND. This task had to identify the sources with a FWHM compatible with the one previously measured and with a minimum emission of photons higher than the one of

the sky, increased by the value of Threshold multiplied by  $\sigma$  (Ciroi, Cracco, Frassati 2011):

$$I_{\min} = I_{\text{sky}} + (\text{Threshold} \times n \times \sigma) \quad (2)$$

Therefore, we used the task TVMARK in order to verify the correctness of the identification of the sources. This task overlaps the found sources, identified by marks, to the image. We made some attempts changing the Threshold and  $n$ -sigma values up to reach a reliable identification of a great number of stars. The values of these parameters are respectively 25 and 6.

With the task PHOT of IRAF we obtained a table for each image (*g*, *r*, *i*), containing the coordinates of the identified sources and the respective instrumental magnitudes. The sources found are 844, 974 and 1248 respectively for the *g*, *r*, *i* filter.

In order to find the same stars in the *g*, *r*, *i* images, we matched the coordinates of the sources, using the software TOPCAT, with the constraint that the centroids of the stars mustn't differ more than 5 pixels. 738 sources resulted coincident (Leonard et al. (1988) identified 685 stars).

From the instrumental magnitudes we calculated the apparent magnitudes *g*, *r*, *i*, using the parameters shown in Table 1 by means the following formulas (Ciroi, Cracco, Frassati 2011):

$$g_{\text{cal}} = g_0 + g - 25 - k_g \times \text{airmass}_g \quad (3)$$

$$r_{\text{cal}} = r_0 + r - 25 - k_r \times \text{airmass}_r \quad (4)$$

$$i_{\text{cal}} = i_0 + i - 25 - k_i \times \text{airmass}_i \quad (5)$$

Then we turned the calibrated magnitudes into the *B*, *V*, *R* magnitudes, which is the standard photometric system of Johnson.

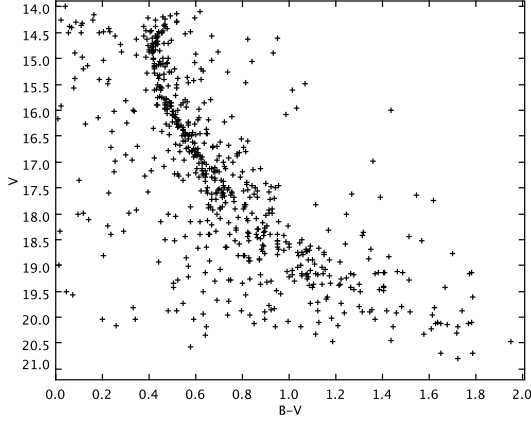
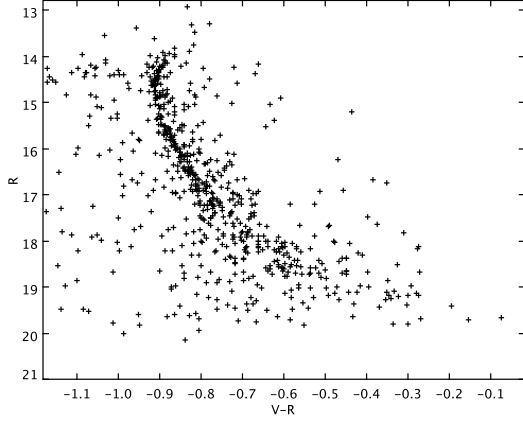
$$B = g_{\text{cal}} + 0.349 \times (g_{\text{cal}} - r_{\text{cal}}) + 0.245 \quad (6)$$

$$V = g_{\text{cal}} - 0.569 \times (g_{\text{cal}} - r_{\text{cal}}) + 0.021 \quad (7)$$

$$R = r_{\text{cal}} + 0.153 \times (r_{\text{cal}} - i_{\text{cal}}) - 0.117 \quad (8)$$

Eventually, we obtained the *B-V* vs *V* and *V-R* vs *R* CMDs by using TOPCAT (Figures 5 and 6).

Since the distance is equivalent for all the stars of the cluster, the apparent magnitudes can be compared as if they were absolute magnitudes. By using TOPCAT, we plotted on the two CMDs some theoretical models (Figures 7, 8 and 9), called isochrones, that describe the distribution of the stars with the same age. Consequently, these models allow us to understand the phases of the stellar evolution, in fact the positions of the stars on the CMD will vary over time. The isochrones we used (Girardi et al. 2004) are given in absolute magnitudes and with reddening-free colours, so the curves must be shifted along the x and y-axis to fit the observational data. The displacement along the y-axis gives us the Distance Modulus ( $DM = V - M_V$ ),


**Fig. 5.** Color-Magnitude Diagram,  $B-V$  vs  $V$ .

**Fig. 6.** Color-Magnitude Diagram,  $V-R$  vs  $R$ .

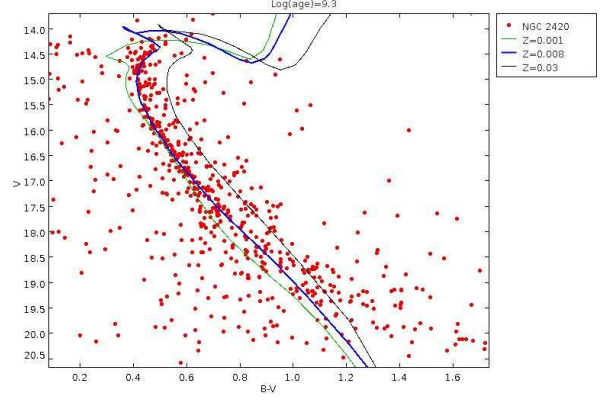
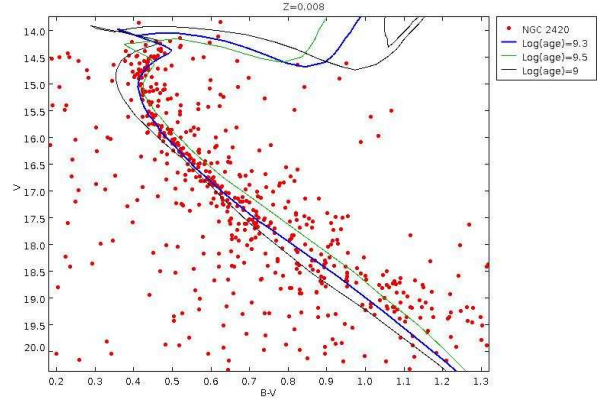
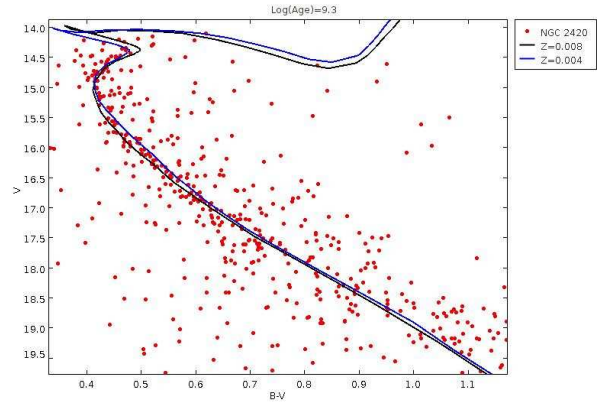
whereas the displacement along the x-axis gives the color excess ( $E(B-V)$ ). Then the interstellar absorption is obtained by means the following formula:

$$A_V = 3.1 \times E(B-V) \quad (9)$$

Once estimated the DM value, we obtained the distance with the formula:

$$d = 10^{\frac{DM+5-A_V}{5}} \quad (10)$$

Each isochron is characterized by a certain metallicity and age. Some attempts were made using the  $B-V$  vs  $V$  CMD. NGC 2420 can be described using various isochrones with different age and metallicity. However, it was possible to exclude some isochrones because they required no absorption at all, or even negative absorption values or, more over, an inconsistent DM. Anyway, being clearly visible the turnoff point, we estimated an age of 2 Gyr, with a DM of about 12.3 and  $E(B-V)$  between 0.07 and 0.16 (Table 4). It is difficult to calculate

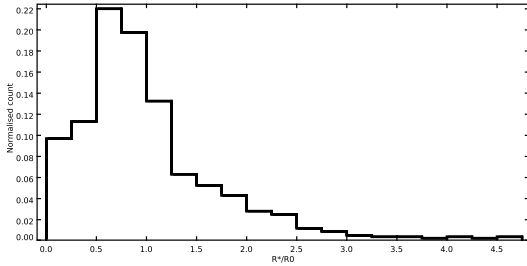

**Fig. 7.** Isochrones with different metallicities and the same age ( $\log(\text{age}) = 9.3$ ) on the  $B-V$  vs  $V$  CMD.

**Fig. 8.** Isochrones with different ages and the same metallicity ( $Z=0.008$ ) on the  $B-V$  vs  $V$  CMD.

**Fig. 9.** Fitting of the two best isochrones on the CMD,  $\log(\text{age}) = 9.3$ ,  $Z=0.004$  (black curve) and  $Z=0.008$  (blue curve).

the exact value of the metallicity only with photometric data, however, a value of  $Z$  between 0.004 and 0.008 can be considered plausible.

In order to provide an estimate of the radii of the stars, we derived the angular radii as a

Z	Log(age)	E(B-V)	DM	A <sub>v</sub>	Distance (pc)
0.030	9.3	0.00	12.1	0	
0.001	9.3	0.25	12.7	0.78	
<b>0.004</b>	<b>9.3</b>	<b>0.16</b>	<b>12.4</b>	<b>0.48</b>	<b>2365</b>
<b>0.008</b>	<b>9.3</b>	<b>0.07</b>	<b>12.3</b>	<b>0.22</b>	<b>2586</b>
0.008	9.5	0.00	11.6	0	
0.008	9.0	0.20	13.2	0.62	

**Table 4.** Parameters obtained by fitting the isochrones with the stellar distribution on the CMD. The isochrones that best fitted the distribution on the CMD are indicated in bold.



**Fig. 10.** Distribution of the radii of the stars ( $R_*/R_\odot$ ), obtained with the surface brightness method.

function of the surface brightness ( $P_v$ ), defined as magnitude per arcsec<sup>2</sup>, employing the formula (Ciroi, Cracco, Frassati 2011):

$$\frac{\Theta_R}{\Theta_R^\odot} = 10^{-2 \times [P_v + 0.1 \times (m_v - m_v^\odot)]} \quad (11)$$

Once determined the angular radius of the star, we could derive the linear radius by using the formula (Ciroi, Cracco, Frassati 2011):

$$\frac{R_*}{R_\odot} = \frac{\Theta_R}{206265} \times \frac{d}{6.96 \times 10^5} \quad (12)$$

where  $d=2475.5$  pc ( $\cong 7.64 \times 10^{16}$  km), it is the average of the distances obtained by the best fits (Figure 9).

The distribution of the radii (Figure 10) shows a mode slightly inferior than solar radius ( $0.75 \times R_\odot \lesssim R_{moda} \lesssim R_\odot$ ). The radius of the stars in the turnoff is between 2 and 3 solar radii (Figure 11).

In this work we used the Z metallicities, while Anthony-Twarog et al. (2006) expressed the metallicity of NGC 2420 as Fe/H (the logarithm of the ratio of the existimated iron abundance of NGC 2420 compared to that of the Sun), that is usually determined spectroscopically. More over, the cited authors obtained two different values of Fe/H because they employed two different techniques. Since we were given the existimated Fe/H values also by the other authors (Demarque et al. (1994), Prada Moroni et al (2001)), we recalculated

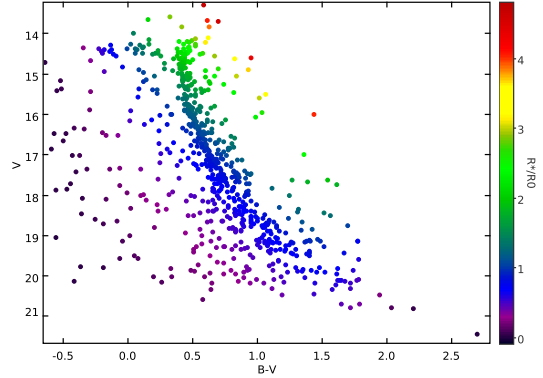


**Fig. 11.** CMD, the radii of the stars are shown with a coloured scale. The radius of the stars at the turnoff is between 2 and 3  $R_\odot$ .

the values of the metallicity of NGC 2420 found in the most recent literature in the light of the new solar metallicity  $Z_\odot=0.0122$  (Asplund et al. 2006) by means the formula:

$$Z = Z_\odot \times 10^{\text{Fe}/\text{H}} \quad (13)$$

The values we obtained are shown in Table 5.

Reference	Z	Z recalculated	Fe/H
1	0.01	0.006	-0.3
2	0.007	0.005	-0.4
3a	na	0.006	-0.32
3b	na	0.005	-0.37

**Table 5.** Metallicity of NGC 2420 according to the original and recalculated bibliographical versions. References: (1) Demarque et al. (1994) - (2) Prada Moroni et al (2001) - (3\*) Anthony-Twarog et al. (2006)

More information on metallicity and on Fe/H can be found here: <http://en.wikipedia.org/wiki/Metallicity>

## 4. Results

We carried out a photometric analysis of the open cluster NGC 2420 starting from three images obtained with the  $g$ ,  $r$  and  $i$  filters, collected from the SDSS archive. The purpose was the determination of the age and the distance of the cluster by means the  $B-V$  vs  $V$  and  $V-R$  vs  $R$  CMDs ( Figures 5 and 6 respectively). These diagrams were compared to the isochrones obtained by the models of Girardi et al. (2004), which enabled us to provide an estimate of the age, distance and metallicity of the cluster. Our CMDs show clearly that NGC 2420 is composed mainly of MS stars and has an evident turnoff. The age of NGC 2420 turned out to be

about 2 Gyr, and the distance about 2475 pc. The determination of its metallicity results very difficult through photometric analysis alone. Nevertheless, the best fit models (Figure 9) give a reasonable value of  $Z$  between 0.004 and 0.008.

References	$E(B-V)$	DM	Age (Gyr)	$Z$
this work	<b>0.16</b>	<b>12.35</b>	<b>2</b>	<b>0.004</b>
this work	<b>0.07</b>	<b>12.28</b>	<b>2</b>	<b>0.008</b>
1	0.05	11.95	2.4	0.006
2	0.08	12.05	2	0.005
3a	0.05	12.15	1.9	0.006
3b	0.05	12.15	1.9	0.005

**Table 6.** Comparison between the results of this work (indicated in bold) and the most recent data. References: (1) Demarque et al. (1994) - (2) Prada Moroni et al (2001) - (3\*) Anthony-Twarog et al. (2006).

By comparing our results with the most recent data collected from the literature, it appears that age and metallicity are consistent with the values found by Demarque et al. (1994), Prada Moroni et al (2001) and Anthony-Twarog et al. (2006) (Table 6). We point out that Anthony-Twarog et al. (2006) strongly support that the metallicity of NGC 2420 is half the solar one ( $Z_{\odot}=0.01$ ). With this value of metallicity all the cited authors obtain a distance slightly lower than ours. Concerning the color excess, we find a reasonable agreement with the literature using  $Z=0.008$ , which is very near the solar metallicity. Finally, we evaluated the stellar radii by means the surface brightness method (Ciroi, Cracco, Frassati 2011), the stellar radii at the turnoff point is between 2 and 3  $R_{\odot}$ . This value is consistent with the age of the cluster.

## References

- Anthony-Twarog, B. J., Delora, T., Cracraft, M., & Twarog, B.A. 2006, AJ, 131, 461-472  
 Asplund, M., Grevesse, N., & Sauval, A. J., 2006, CA, 147, 76-79  
 Giroi, S., Cracco, V., Frassati, A., 2011, Fotometria, 'the Sky as a Laboratory', handouts, 101  
 Demarque, P., Sarajedini, A., & Guo, X.-J., 1994, AJ, 426, 165-169  
 Girardi, L., Greber, E.K., Odenkirchen, M., & Chiosi, C. 2004, apj, 700, 1816  
 Leonard, P. J. T., 1988, AJ, 95, 1  
 Prada Moroni, P. G., Castellani, V., Degl'Innocenti, S., Marconi, M., 2001, Mem. S.Alt., 72, 4